Application of fractional calculus to polarization dynamics in solid dielectric materials
by Gary William Bohannan

A dissertation submitted in partial fulfillment of the requirements for the degree of Doctor of Philosophy in Physics
Montana State University

Abstract:
The fractional calculus has been suggested as an appropriate mathematical tool for the description of a wide variety of physical, chemical and biological processes, in particular non-Debye relaxation in dielectrics. While there have been substantial improvements in our understanding of the physical interpretation of the results of fractional differential equations, there is still much unknown. There is, as yet, not even complete agreement over the notation to be used, let alone the underlying definition of the fractional derivative.

This dissertation explores the hypothesis that there must be an intimate relation between the ac and dc response in any given material represented by a dynamical equation of motion. That at least one of the forms of the fractional calculus does, in fact, provide a useful and practical tool for describing some of the dynamics of immediate interest is demonstrated. The process investigated is that of polarization dynamics in condensed matter dielectric materials. The dielectric material studied in detail is poly(vinylidine fluoride) (PVDF) which finds use in piezoelectric sensor and actuator applications. A dynamical model, based on the fractional calculus, is shown to reproduce both the ac and dc responses to an applied electric field.

Many of the results are directly applicable a wide range of other dynamics including mechanical relaxation processes.

APPLICATION OF FRACTIONAL CALCULUS TO POLARIZATION DYNAMICS IN SOLID DIELECTRIC MATERIALS

by

Gary William Bohannan

A dissertation submitted in partial fulfillment
of the requirements for the degree

of

Doctor of Philosophy

in

Physics

MONTANA STATE UNIVERSITY
Bozeman, Montana

November 2000

APPROVAL

of a dissertation submitted by

Gary William Bohannan

This dissertation has been read by each member of the dissertation committee and has been found to be satisfactory regarding content, English usage, format, citations, bibliographic style, and consistency, and is ready for submission to the College of Graduate Studies.

George F. Tuthill _____ 11/15/00
(Signature) Date

Approved for the Department of Physics

John C. Hermanson _____ 11-15-00
(Signature) Date

Approved for the College of Graduate Studies

Bruce R. McLeod _____ 11-16-00
(Signature) Date

STATEMENT OF PERMISSION TO USE

In presenting this dissertation in partial fulfillment of the requirements for a doctoral degree at Montana State University, I agree that the Library shall make it available to borrowers under rules of the Library. I further agree that copying of this dissertation is allowable only for scholarly purposes, consistent with "fair use" as prescribed in the U. S. Copyright Law. Requests for extensive copying or reproduction of this dissertation should be referred to Bell & Howell Information and Learning, 300 North Zeeb Road, Ann Arbor, Michigan 48106, to whom I have granted "the exclusive right to reproduce and distribute my dissertation in and from microform along with the non-exclusive right to reproduce and distribute my abstract in any format in whole or in part."

Signature Mary William Bohannon

Date November 15, 2000

ACKNOWLEDGEMENTS

With great appreciation for the assistance from fellow graduate and undergraduate students who participated in the development and execution of the experiments crucial to this work: Darin Arbogast, Michael Chase, Jil Hallenberg, Michelle Lindmier, Erica McKenzie, and Delphine Medicine Horse.

I am especially grateful to Recep Avci and Sara Maccagnano for allowing me to participate in their study of anomalous diffusion.

This work was supported by a Montana Space Grant Fellowship, NASA EPSCoR Grant NCC5-240, and NSF Grant DMR-9805272.

TABLE OF CONTENTS

LIST OF TABLES viii

LIST OF FIGURES ix

1. INTRODUCTION 1

2. PROBLEM STATEMENT AND HYPOTHESIS 7

Example Application 8
The Permittivity 9
Permittivity of Dilute Dipolar Liquids 11
Permittivity of Solid Dielectrics 12
Equivalent Circuits 15
Other Proposed Symmetric and Asymmetric Permittivity Functions 17
Low-Frequency, Long-Time Anomalies 20
Polarization versus Conductivity 22
From Whence the Power-law? 23
Hypothesis 25

3. THE MODEL 27

Polarization and Conduction as Statistical Quantities 27
A Statistical Digression 28
Polarization 30
Conductivity 31
Competition and Mixing 32
Distributions of Relaxation Times 33
A Plethora of Models? 34

4. THE FRACTIONAL CALCULUS 35

The Definition of the Fractional Derivative 36
Causality and Time Inversion 41
Fractional Derivative of a Sinusoid 41
Fractional Relaxation 42

5. DERIVATION OF THE DIFFERENTIAL EQUATION 46

The Permittivity Equation 47
Applying the Fractional Calculus to Non-exponential Processes 48
Development of a Differential Equation 49
A Fractional Form of the Constitutive Equation 50

A Second Fractional Form of the Constitutive Equation 54
An Alternative View of the Models 58
Assumption Regarding Initial Conditions 59
Disclaimer 59

6. COMPUTATIONAL METHOD 61

Development of a Numerical Integration Scheme 63
Grünwald Algorithm 64
Direct Integration 66
Example *ac* Reconstruction 68
Spectrum of Response and Noise Masking 69
Example Pulsed *dc* Reconstruction 71
Stepwise Integration 75

7. EXPERIMENTAL METHODS AND RESULTS 80

Material Studied 80
Equipment 81
Sample Holder for Varying Temperature 82
Faraday Cage for Low Frequency Measurements 82
ac Measurements 83
Transient Response Measurement 83
Data Analysis 85

8. OTHER APPLICATIONS AND FUTURE QUESTIONS 98

Extending the Dynamic Range 98
NMR Relaxation Times 99
Domain Wall Relaxation and Self-Pinning 99
Where is the Charge? 100
Application to Mechanical Systems 101
$PI^{\lambda}D^{\mu}$ Control Systems 102
Boundaries and Barriers 104
Many Body Dynamics 104
Relation to Generalized Thermodynamics 105
Fractional versus Fractal 105
Quantum Mechanical Treatment 106
1/f Noise in Resistors 107

9. SUMMARY AND SIGNIFICANCE 108

Lesson Learned 108
Conclusion 110

APPENDICES 111

APPENDIX A – α-STABLE DISTRIBUTIONS 112
The Law of Large Numbers and the Central Limit Theorem 113
Lévy Distributions 114
Diffusion and Drift 118
APPENDIX B – ANOMALOUS DIFFUSION 120
Properties of Normal and Anomalous Diffusion 121
Surface Diffusion of PDMS 123
Surface Diffusion of Cocaine 125
Statistical Implications 128

REFERENCES CITED 130

LIST OF TABLES

Table Page

1. Relations Between the Four Basic Immitance Functions 10

2. Spectral Functions and Their Power-Law Exponents 19

3. Simulated measurements of complex permittivity at 10 kHz for varying delay times 69

LIST OF FIGURES

Figure Page

1. A schematic representation of the real, ϵ', and imaginary, ϵ'', parts of the complex permittivity as predicted by the Debye model 11

2. A schematic representation of ϵ'' versus ϵ' as predicted by the Debye model 12

3. A schematic representation of the real, ϵ', and imaginary, ϵ'', parts of the complex permittivity as predicted by the Cole-Cole model 13

4. A schematic representation of ϵ'' versus ϵ' as predicted by the Cole-Cole model 13

5. A comparison of the real, ϵ', parts of the complex permittivity as predicted by the Debye and Cole-Cole models 14

6. A comparison of the imaginary, ϵ'', parts of the complex permittivity as predicted by the Debye and Cole-Cole models 14

7. Equivalent circuits for (a) the Debye model and (b) the Cole-Cole model 16

8. Comparison of the loss tangent for the Debye and Cole-Cole Models.... 17

9. A schematic representation of a typical data set from measurements of a ferroelectric material 20

10. Hopping Model 31

11. Linear plot of weights associated with the fractional derivative for $q = 0.5$ 39

12. Logarithmic plot of the absolute value of the weights associated with the fractional derivative for $q = 0.5$. The time scale shown here is 15 times longer than that shown in Figure 11 39

13. Time domain decay of polarization for various values of the exponent q 44

14. Nb-doped (1 at. %) Remeika ($BaTiO_3$) single crystal. Fit to Equation 5.10 with parameters: $\epsilon_s = 19.4 \times 10^3$, $\delta = -0.11$, $\epsilon_\infty = 6 \times 10^3$, $\mu = 0.79$, $\epsilon_c = 60$, $\beta = -0.795$, $q = 0.977$, $\tau = 8.8 \mu$sec. Data point labels are in kHz. Solid lines drawn as aids to the eye..... 53

15. The noise power spectrum predicted from Figure 14. A line with 1/f shape is drawn to demonstrate how close the predicted noise spectrum is to 1/f behavior in the anomalous conduction region. Solid line drawn as an aid to the eye..... 54

16. An ideal element RC circuit incorporating conductivity..... 55

17. Nb-doped (1 at. %) Remeika ($BaTiO_3$) single crystal. Fit to Equation 5.13 with parameters: $\epsilon_s = 25.2 \times 10^3$, $\epsilon_\infty = 1.5 \times 10^3$, $\epsilon_c = 1.1 \times 10^3$, $q = 0.76$, $\beta = -0.5$, $\nu = 0.26$, $\tau = 12.06 \mu$sec. Data point labels are in kHz. Solid lines drawn as aids to the eye. Note that the values of parameters vary from those in Figure 14..... 57

18. A time domain simulation reconstructing the response to a 10.0 kHz field using the parameters of Figure 14..... 68

19. Figure 14 with ϵ^* values computed from simulation by numerical integration of Equation 6.13..... 70

20. The computed power spectrum of Figure 18 with no noise..... 70

21. The computed power spectrum of Figure 18 with 0.1% rms noise applied to the electric field..... 71

22. Polarization decay curves resulting from pulses of varying duration. The toy system has a time constant $\tau = 0.1 sec$. Curve (1) is decay after pulse of 40 τ, curve (2) after pulse of 120 τ, curve (3) after pulse of 600 τ. Curve (4) is the fractional relaxation curve predicted by Equation 4.16..... 72

23. A time domain simulation reconstructing the response of the second toy system to a pulse 200 seconds (2000 τ) in duration. The exponent $\delta = -0.1$ for this case..... 74

24. Comparison of relaxation currents in the second toy system; (1) during application of an external field and (2) after it is removed..... 75

25. A time domain simulation reconstructing the response of the first toy system to a pulse of $\sim$ 5.5 sec. Memory retention limited to 30 seconds 79

26. An enlargement of the response around the $t = 30$ second time-frame from Figure 25 above showing the pulse echo resulting from truncating the memory. Duration of memory is 30 seconds in this simulation 79

27. The sample holder and LN2 cryogenic chamber 83

28. A schematic of the experimental setup for measuring *ac* permittivity ... 84

29. A schematic of the experimental setup for measuring transient response 84

30. Cole-Cole plot for PVDF sample #1 at 295 K. Note the slight offset of the data point at 50 kHz 87

31. Cole-Cole plot for PVDF sample #1 at 315 K. The resonance loop at 50 - 60 kHz is well developed 87

32. Cole-Cole plot for PVDF sample#1 at 325 K. The resonance loop is even more developed 88

33. Cole-Cole plot for PVDF at 305 K. After cooling from 325 K, the resonance loop has been suppressed 88

34. Cole-Cole plot for PVDF sample #2 (4.7 cm $\times$4.7 cm) at room temperature 89

35. Parameter fit for PVDF sample #2 at room temperature. The time constant is $\tau = 173$ ns, the exponents $q = 0.603$ and $\nu = 0.524$ and the coefficients $\epsilon_\infty = 3.75, \epsilon_s = 9.32, \epsilon_c = 0.465$. The underlying exponents of the model are $\alpha = 0.397$ and $\gamma = 0.921$. The model has been extrapolated to very low frequency 90

36. Universal dielectric response display for PVDF. The exponent derived from this plot is $1 + \lambda = 0.9777$ 91

37. Predicted charging and discharging currents for PVDF sample #2 at room temperature using Equation 5.13 and the parameters from Figure 35. The two asymptotic exponents are also shown. Current in amps is found by multiplying the displayed value by $C_c\times$ Voltage 92

38. Real and imaginary parts of measured permittivity of sample #8 at room temperature showing the resonance between 5 and 12 kHz 94

39. Predicted charging and discharging currents for PVDF sample #8, 2 × (9.6 cm × 9.6 cm), at room temperature. From Figure 37 95

40. Measured discharging currents for PVDF sample #8, 2 × (9.6 cm × 9.6 cm), at room temperature. Solid and dashed lines are predicted values, symbols are measured data 95

41. Comparison of an α-stable distribution of $\alpha = 1.8$ with a Gaussian. Both have $\sigma = 1.0$. Note the slightly greater emphasis at the center of the distribution. The X marks on the graph indicate the relative number of events outside $\pm 5\ \sigma$ for the $\alpha = 1.8$ case 116

42. Measured and simulated diffusion of PDMS. In (a), from top, the images were recorded at 12, 27 and 88 minutes. In (b), from top, the simulation results were recorded after 6, 48, and 234 jumps..... 124

43. Measured and simulated diffusion of cocaine. Note that the sharp edges remain in both the measurements and simulation. Due to the ability of the TofSIMS to detect the surface layer only, the actual density differences between the lay down region and the open surface are more likely to be that shown in the fourth column. The density in the open substrate area is almost imperceptible compared to the amount retained in the original deposition region 127

44. Comparison of the Lévy, or α-stable, ($\alpha = 0.01$) and Gaussian distributions in the cross-over regime 128

ABSTRACT

The fractional calculus has been suggested as an appropriate mathematical tool for the description of a wide variety of physical, chemical and biological processes, in particular non-Debye relaxation in dielectrics. While there have been substantial improvements in our understanding of the physical interpretation of the results of fractional differential equations, there is still much unknown. There is, as yet, not even complete agreement over the notation to be used, let alone the underlying definition of the fractional derivative.

This dissertation explores the hypothesis that there must be an intimate relation between the *ac* and *dc* response in any given material represented by a dynamical equation of motion. That at least one of the forms of the fractional calculus does, in fact, provide a useful and practical tool for describing some of the dynamics of immediate interest is demonstrated. The process investigated is that of polarization dynamics in condensed matter dielectric materials. The dielectric material studied in detail is poly(vinylidine fluoride) (PVDF) which finds use in piezoelectric sensor and actuator applications. A dynamical model, based on the fractional calculus, is shown to reproduce both the *ac* and *dc* responses to an applied electric field.

Many of the results are directly applicable a wide range of other dynamics including mechanical relaxation processes.

CHAPTER 1

INTRODUCTION

This dissertation focuses on the application of the fractional calculus to the problem of describing polarization dynamics in dielectric materials. The use of fractional calculus for this purpose has been suggested in the literature but not thoroughly investigated. In particular, the investigation focuses on the requirement that there must be an intimate relation between the *ac* and *dc* response in any given material represented by a dynamical equation of motion.

In order to appreciate the statistical interpretation of the results, a discussion of the problem of anomalous surface diffusion has been included as an appendix. This will allow comparison and contrast between the study of bulk behavior and individual particle behavior.

Polarization dynamics in ferroelectric materials, as in all dielectrics, pose a very complicated problem. Among the complications is the fact that the relaxation response is rarely, if ever, a simple exponential function as described by Debye. [1] Instead a fractional power exponential decay (the "stretched exponential") of the form

$$\phi(t) = \phi_0 \exp\left(-\left(\frac{t}{t_0}\right)^{\alpha}\right), \tag{1.1}$$

with $0 < \alpha < 1$, or power law of the form

$$\phi(t) \approx \left(\frac{t}{t_0}\right)^{-\alpha}, \tag{1.2}$$

at long times, again with $0 < \alpha < 1$, are far more common, to the point of being referred to as universal responses.

Additionally, at very "low" frequencies, or "long" times, the relaxation current flowing after application of an external field, the "charging current," follows a power law of the form

$$i(t) \approx \left(\frac{t}{t_0}\right)^{-n}, \tag{1.3}$$

with $0 < n < 1$. Although many articles in the literature are ambiguous on this point, it appears to be "universally" true that the "discharging" current follows a different power-law relation than the "charging" current. What is common is that there are power-law relations involved in both cases.

Dielectric materials share these non-Debye relaxation responses with mechanical systems that exhibit non-exponential strain relaxation after removal of an external stress and power-law creep under continuous stress. Fractional power-law behavior is the norm in condensed matter dynamics. To quote Ngai:

> The relaxation phenomena ... include relaxation, a.c. conductivity, creep, stress relaxation, internal friction, relaxation observed through photon correlation spectroscopy, nuclear magnetic resonance relaxation, spin-echo measurements, transient capacitance (i.e. time resolved) electrical transport, transient optical luminescence, volume and enthalpy relaxation and recovery, differential scanning calorimetry, steady flow viscosity,

> stress-strain relationship and its dependence on strain-rate, ultrasonic attenuation, noise, diffusion, diffusion controlled chemical reactions and electronic recombination, etc. Materials involved include liquids, supercooled liquids, inorganic glasses, electrolytes, ionic conductors, dielectrics, gate insulators of electronic devices, amorphous semiconductors, xerographic materials, polymer melts and solutions, amorphous polymers, rubbers, plastics, epoxies, metals, ... ceramics, piezoelectrics, pyroelectrics, ferroelectrics, biopolymers, ... etc. The wealth of physics, the number of interesting physical phenomena are staggering. [2]

By focusing on non-exponential response functions, this work gains a broad applicability to many problems in condensed matter physics. The intent is to improve our understanding of this universal behavior in order to better understand complex dynamics in a wide variety of condensed matter systems.

Traditionally, the broad relaxation spectra, i.e. relaxation rates encompassing nine or more decades of frequency, have been described as resulting from a linear combination of exponential responses with an extremely large distribution of time constants (e.g. see [3]). This "distribution of exponential time constants" description has been used extensively as it relies on traditional concepts of weakly interacting systems with a wide range of simple exponential relaxation mechanisms.

The debate between the distribution of relaxation times (DRT) and power-law points of view has abated with the two views now being virtually complementary, at least for the frequency regime around the dielectric loss peak. The fact of power-law behavior has been incorporated into texts such as Reference [4], which extensively cites early works on power-law behavior, e.g. References [5, 6, 7, 8], while still using the DRT description to flesh out physical models when appropriate. The DRT approach

was incorporated into a simulation model in Reference [9], and has been recently been posed in terms of multifractals in Reference [10], for example.

Hill and Jonscher [11] suggested that the power-law behavior is a result of the many-body interactions within bulk condensed matter. Funke [12] offered a reasonable model for the interactions. Funke's model can be generalized to cover a broad range of behaviors, even those that Funke discarded in his paper. It is somewhat ironical that an argument based on distributions of relaxation times may provide the most direct route to power-law behavior.

What has been missing is a coherent dynamical model, even a phenomenological one, that allows both the steady state *ac* response and the transient *dc* response to be included in one composite whole over all relevant frequency and time scales. Such a model would be a great boon to both the basic characterization of materials and to the problem of developing control systems to apply materials to applications. The thrust of this dissertation is to examine the hypothesis that the power-law description is fundamental and covers a broad range of measured phenomena. The hypothesis includes the statement that the fractional calculus is appropriate and tractable for use in describing power-law dynamics.

The problem of anomalous diffusion is related to that of relaxation dynamics in a very deep sense. The motion of individual charge carriers making up an electronic or ionic current is, after all, a diffusive process. There are some substantial differences, however, in the underlying causes of power-law dynamics in super-diffusive versus

sub-diffusive processes. Sorting out these similarities and differences is crucial to understanding dynamics in materials.

As will be discussed in subsequent chapters, power-law processes are fundamentally non-Markovian and pose a number of very substantial theoretical and computational difficulties. Approaches for dealing with several of these difficulties are presented in the context of solid state dielectric materials, but the results could be applied to a wide range of problems in mechanical and biological systems as well. A computational method for simulating power-law dynamics through the use of fractional difference equations is presented in detail in this thesis.

A major difficulty remains, however. The language of physics is ill-equipped to deal with non-Markovian processes. The term "initial conditions" is moot; these conditions incorporate all of history. Also, processes which produce power-law-like behavior are often assumed to be nonlinear. The dynamical equations derived in subsequent chapters are first order in the dynamical variables and the fractional derivative is a linear operator. So, in what sense are these systems linear or nonlinear?

Chapter 2 describes the dielectric relaxation problem in more detail and formally states the hypothesis that the fractional calculus provides a workable description of the dynamics. Chapter 3 develops the generalized micro- and macroscopic model of many-body interactions leading to non-Debye behavior.

Chapter 4 provides an overview of the fractional calculus and its application to the problem of non-exponential response. In Chapter 5 time domain fractional differential

equations are derived from *ac* response measurements. Two methods for integrating the differential equation are derived in Chapter 6, and verification testing results are presented. Chapters 5 and 6 represent the major theoretical and computational contribution to the field of non-Debye relaxation dynamics.

In Chapter 7, experimental methods for characterizing the polarization response under varying external field conditions are discussed. Permittivity measurements are used to predict transient currents. This connection between the *ac* and *dc* measurements demonstrates the validity of the hypothesis.

Chapter 8 outlines possible extensions of the research into other areas of interest as well as discussing several open questions related to the understanding of fractional dynamics. Chapter 9 provides a summary of the results and conclusions.

Appendix A provides details of the generalized central limit theorem and a brief discussion of the statistics of anomalous drift and diffusion.

Appendix B explores the use of the fractional calculus to the description of anomalous diffusion. A simulation model is developed which reproduces both "normal" and extremely anomalous surface diffusion. One of the objectives of including this appendix is to clarify the differences between the coarse grained modeling used in the earlier chapters for description of polarization dynamics and detailed modeling of individual particle behavior.

CHAPTER 2

PROBLEM STATEMENT AND HYPOTHESIS

A direct consequence of the Kramers-Kronig relations is that the ideal dielectric, i.e. lossless over all frequencies, violates causality and cannot exist. If the ideal capacitor model with impedance $Z = 1/i\omega C$ is not physical, what description should we use? In general, we are looking for constitutive equations of the form $\mathbf{D} = \epsilon\mathbf{E}$. If the ideal capacitor model isn't physically possible, then ϵ cannot be independent of frequency. A number of models dating back to Debye [1] have been proposed, but we should evaluate the models on their ability to reproduce the measured dynamics of materials and devices. This issue arises in mechanical systems as well, in fact, in any system capable of storing energy.

This work will be focused on the dynamical response of solid dielectric materials to an external electric field, using the methods of impedance spectroscopy. The problem originates in the need to characterize the dynamic response of materials that may ultimately be used in devices and systems, as well as in the desire to understand fundamental properties of condensed matter. This chapter provides background on traditional attempts to develop permittivity models and proposes a hypothesis for development of future models.

Example Application

Of specific interest is the problem of obtaining effective, efficient control of piezoelectric materials for applications such as actuators and sensors. [13, 14, 15] Piezoelectric properties are usually addressed in terms of displacement, or strain, per unit voltage, or electric field, applied [16]. In the particular application of interest, vibration isolation in space applications, operating high voltage amplifiers in the linear mode is unacceptably wasteful of power due to losses in the amplifiers themselves.

Since the poly(vinylidine fluoride) (PVDF) used as the piezoelectric material has an exceedingly small rated *dc* conductivity, as do most popular piezoelectrics, it would be much more efficient to operate the devices with pulsed charge-pump type circuits and use the PVDF actuator material itself as a capacitor in the charging system. Here the problem becomes one of refining the linear approximation between charge and voltage, $Q = CV$. The direct, linear relation between the electric field, $\mathbf{E}$, and the electric displacement, $\mathbf{D}$, no longer holds if the capacitance changes with time and frequency. [17]

The problem will only become more difficult with the advent of high-strain piezoelectric materials such as those reported in Reference [18]. These exhibit a definite nonlinear response in strain versus field. We must expect that the strain and dielectric properties of these materials will show time and frequency dependence as well as nonlinearity with respect to applied field.

The Permittivity

Impedance spectroscopy is a method of characterizing many of the electrical properties of materials and their interfaces with electrically conducting electrodes. It can be used to investigate the dynamics of bound or mobile charges in the bulk or interfacial regions of solid or liquid material. Of principal interest is the complex permittivity function $\epsilon^*(\omega) = \epsilon'(\omega) - i\epsilon''(\omega)$, which is the *steady state ac* response of the polarization to an applied external field. We will consistently be referring to the relative permittivity as the permittivity. In MKSA units, the polarization and electric displacement are related to the electric field through the constitutive equations

$$\mathbf{P} = \chi_e \epsilon_0 \mathbf{E}, \tag{2.1}$$

and

$$\mathbf{D} = (1 + \chi_e)\epsilon_0 \mathbf{E} = \epsilon\epsilon_0 \mathbf{E}, \tag{2.2}$$

where χ_e is the *electric susceptibility.* In this notation $\epsilon\epsilon_0$ represents the *absolute permittivity.*

The permittivity is related to other response functions, such the impedance, according to Table 1 via the current to displacement relation

$$i = \frac{\mathrm{d}}{\mathrm{dt}} D(t). \tag{2.3}$$

These functions are also referred to as "spectral" functions.

Table 1. Relations Between the Four Basic Immitance Functions.

	Modulus (M)	Impedance (Z)	Admittance (Y)	Permittivity (ϵ)
M	M	μZ	μY^{-1}	ϵ^{-1}
Z	μ^{-1}M	Z	Y^{-1}	$\mu^{-1}\epsilon^{-1}$
Y	μM	Z^{-1}	Y	$\mu\epsilon$
ϵ	M^{-1}	μ^{-1}Z^{-1}	μ^{-1}Y	ϵ

$\mu = i\omega C_C$, where C_C is the capacitance of the empty cell.

To be precise, the displacement, as defined in Equation 2.3, is actually proportional to the total integrated current through the material, rather than the charge accumulated across the material. There is much interest in removing the *dc* conductivity, σ, from the permittivity function in order to write the static contribution to the current as $i = \sigma \mathbf{E}$. This would allow one to determine the charge stored across the dielectric versus that lost to conductivity. One of the objectives of dielectric spectroscopy is to determine the bound charge density, ρ_b, and the free charge density, ρ_f. As will be seen, this is not as straightforward a process as one would desire.

Given that $\mathbf{P}$ and $\mathbf{D}$ differ by the ratio $\chi/(\chi+1)$, with $\chi \geq 10$ for many dielectrics of interest, there is a tendency to use the term "polarization" when "displacement" would be more precise. This difference is washed out even more when considering the fact that materials and measurements can vary by 10% or more. In what follows, we will follow this convention that the term polarization refers to the total integrated current unless specifically noted otherwise. Additionally, in scaling for numerical modeling, the MKSA scale factor ϵ_0 will be set to unity.

Permittivity of Dilute Dipolar Liquids

Debye [1] developed the theory of dielectric relaxation of polar molecules in a viscous medium. In the materials he studied, the concentrations were low enough to appropriately approximate the molecules as non-interacting dipoles. Equation 2.4 expresses the relation in terms of ϵ_s, the low frequency limiting value, and ϵ_∞, the high frequency limiting value, and τ, a characteristic reorientation time for a single dipole.

$$\epsilon^* - \epsilon_\infty = \frac{\epsilon_s - \epsilon_\infty}{1 + i\omega\tau} \quad \text{(Debye)} \tag{2.4}$$

The real, ϵ', and imaginary, ϵ'', are shown in Figure 1. A plot of ϵ'' versus ϵ' is shown in Figure 2 and is used as a standard display of the same information.

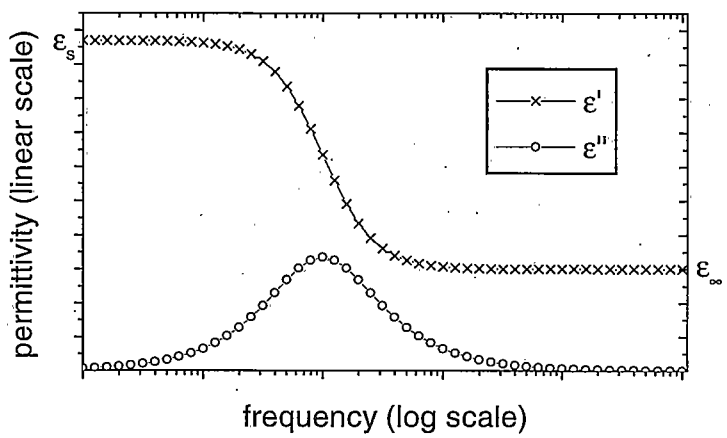

Figure 1. A schematic representation of the real, ϵ', and imaginary, ϵ'', parts of the complex permittivity as predicted by the Debye model.

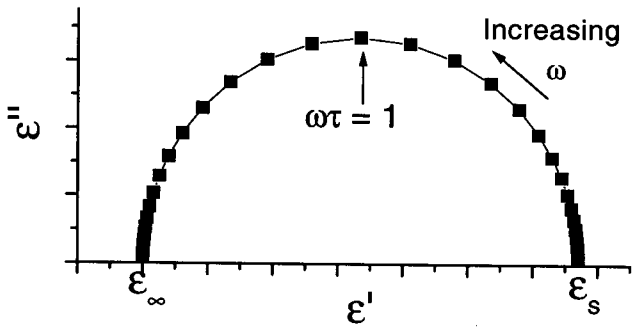

Figure 2. A schematic representation of ϵ'' versus ϵ' as predicted by the Debye model.

Permittivity of Solid Dielectrics

In dielectric solids, the assumption of non-interacting dipoles breaks down and the simple relaxation function of the Debye model is no longer adequate. Cole and Cole [3] found that, at least for a range of frequencies around the loss peak, the permittivity data for non-dilute materials looked more like that shown in Figure 3. When plotted as ϵ'' versus ϵ', they noted that the result was a circular arc with the center below the real axis as depicted in Figure 4.

By appeal to purely geometric arguments they developed the following form for the permittivity function:

$$\epsilon^* - \epsilon_\infty = \frac{\epsilon_s - \epsilon_\infty}{1 + (i\omega\tau)^{1-\alpha}} \quad \text{(Cole-Cole)} \tag{2.5}$$

where the exponent parameter α is determined from the depression of the center of the circular arc below the real axis. In fact, $\alpha\pi/2$ is the angle of offset of the center of the arc with respect to the real axis. The meaning of ϵ_s and ϵ_∞ remain as for the Debye case, but the time constant τ and the exponent parameter α need additional

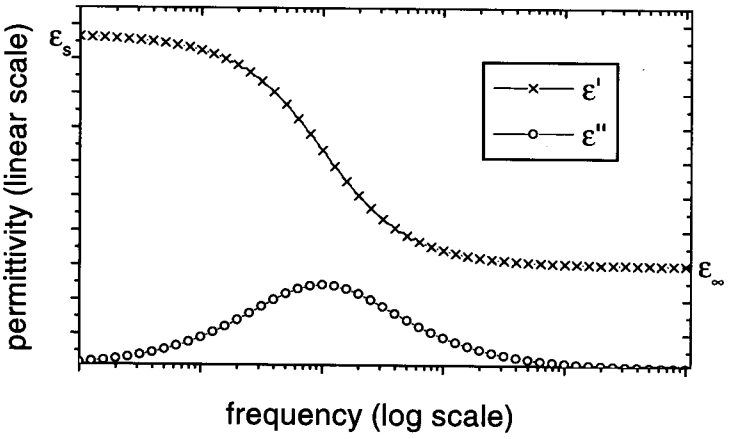

Figure 3. A schematic representation of the real, ϵ', and imaginary, ϵ'', parts of the complex permittivity as predicted by the Cole-Cole model.

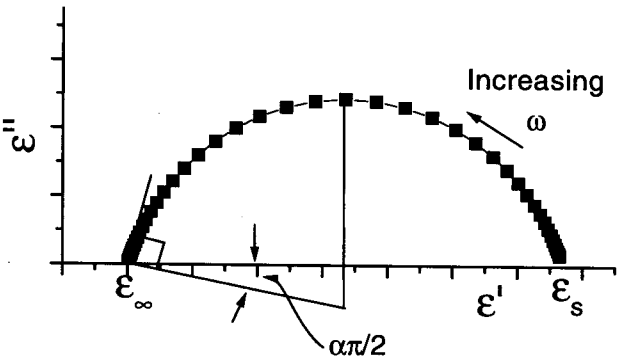

Figure 4. A schematic representation of ϵ'' versus ϵ' as predicted by the Cole-Cole model.

physical interpretation. Since Cole and Cole made the plot of ϵ'' versus ϵ' popular, it is now often referred to as a "Cole-Cole" plot regardless of whether or not the data fit Equation 2.5.

The differences between the Debye and Cole-Cole models become more dramatic when displayed together in a log-log scale as in Figures 5 and 6. The loss peak for the Cole-Cole model is broader than that predicted by the Debye model.

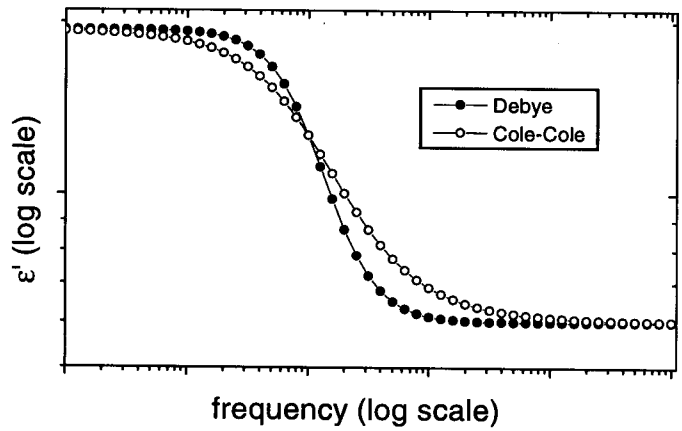

Figure 5. A comparison of the real, ϵ', parts of the complex permittivity as predicted by the Debye and Cole-Cole models.

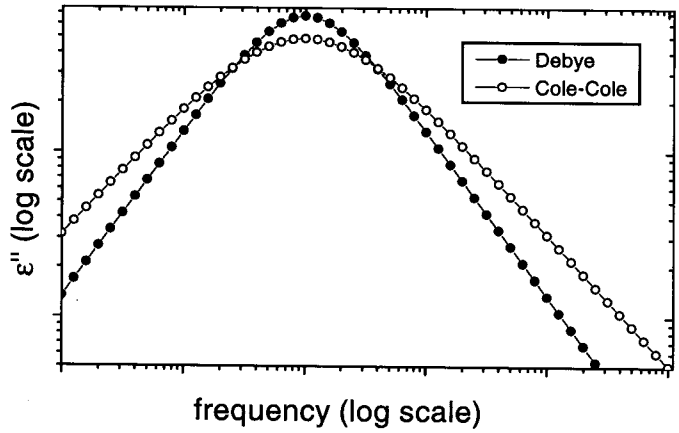

Figure 6. A comparison of the imaginary, ϵ'', parts of the complex permittivity as predicted by the Debye and Cole-Cole models.

The distribution of time constants idea is based on the assumption of a superposition of many linear relaxation processes contributing to the permittivity. In general:

$$\epsilon^* - \epsilon_\infty = \int_0^\infty \frac{(\epsilon_s - \epsilon_\infty)G(\tau)\mathrm{d}\tau}{1 + i\omega\tau} \tag{2.6}$$

where $G(\tau)$ represents a normalized distribution of relaxation times. For the Cole-Cole model:

$$G(\tau) = \frac{1}{2\pi\tau} \frac{\sin \alpha\tau}{\cosh(1-\alpha)\log(\tau/\tau_0) - \cos \alpha\tau} \tag{2.7}$$

The distribution is even with respect to a central frequency, but other distributions need not be. A more detailed analysis of distribution functions for non-Debye relaxation processes can be found in Reference [10].

In the time domain, Cole-Cole relaxation is best fit with a "stretched exponential" function at short to intermediate times (compared to τ) and asymptotically with a power law at very long times. The difficulty in making consistent decay measurements is that materials generally exhibit memory of past polarization. [19] This effect will be addressed in detail in Chapters 6 and 7.

Equivalent Circuits

An equivalent circuit for the Debye model is shown in Figure 7a. The circuit parameters are related to the measured ϵ values as follows:

$$\mathrm{C}_\infty = \epsilon_\infty \mathrm{C}_\mathrm{c}, \quad \mathrm{C}_\mathrm{s} = (\epsilon_s - \epsilon_\infty)\mathrm{C}_\mathrm{c}, \quad R_\mathrm{s} = \frac{\tau}{\mathrm{C}_\mathrm{s}} \tag{2.8}$$

where τ is the reciprocal of the angular frequency of the loss peak and C_c is the capacitance of the empty test cell.

Cole and Cole proposed the equivalent circuit shown in Figure 7b and introduced the concept of the "constant phase element" (CPE). This label was given to the new

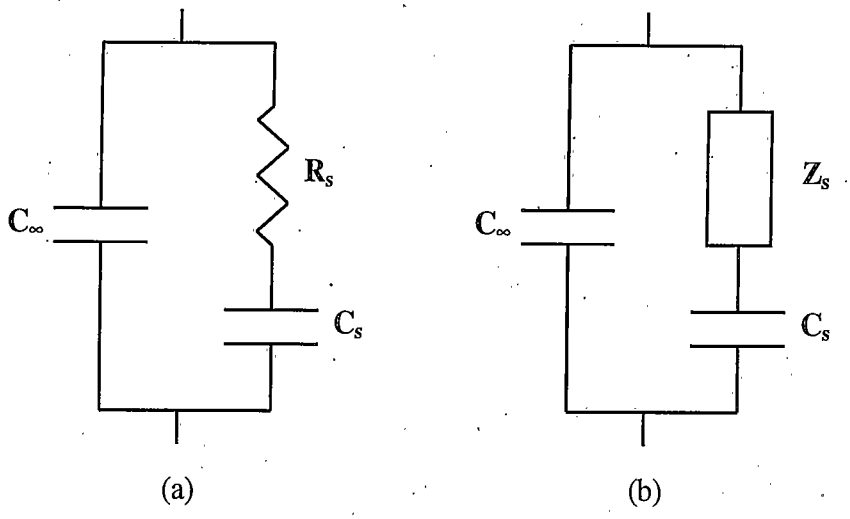

Figure 7. Equivalent circuits for (a) the Debye model and (b) the Cole-Cole model.

frequency dependent "lossy" element, Z_s, because it produced a nearly constant phase shift, and a nearly constant loss tangent ($\tan\delta = \epsilon''/\epsilon'$), over a large frequency range. The energy lost per cycle is nearly independent of frequency. The loss tangent is not strictly constant. The term originated from the fact that the variation in ϵ'' is dramatically less than that predicted by the Debye model as is evident in Figure 6. A comparison of the loss tangents for the two models is shown in Figure 8. Why the variation in the loss tangent should be suppressed was left as an open question by Cole and Cole.

The element Z_s is related to the measured values by:

$$Z_s = \frac{\tau(i\omega\tau)^{-\alpha}}{C_s}. \tag{2.9}$$

It is evident that, for $0 < \alpha < 1$, the element Z_s is neither a resistor nor a capacitor, but some mixture of the two. Distributed arrays of conventional ideal resistors and

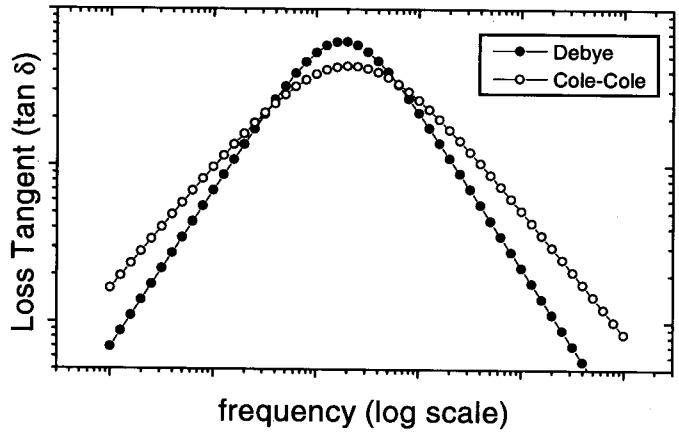

Figure 8. Comparison of the loss tangent for the Debye and Cole-Cole Models.

capacitors that produce the CPE properties have been proposed, e.g. Reference [4] and Reference [9].

Other Proposed Symmetric and Asymmetric Permittivity Functions

Not all dielectric loss peaks display the symmetry of the Cole-Cole equation in the log-log plot of ϵ'' versus ϵ'. A number of variations on Equation 2.5 have been proposed to provide better parametric fit to the data obtained from experiment.

These functions generally include terms of the form $\epsilon^* - \epsilon_\infty$ and $\epsilon_s - \epsilon_\infty$, in which the assumption is made that there is a polarization response in the material at the highest frequencies of interest,

$$\epsilon_\infty - 1 = \mathbf{P}_\infty / \epsilon_0 \mathbf{E}. \tag{2.10}$$

The "infinite" frequency is typically in the microwave region or below.

In Table 2, taken from Reference [11], Hill and Jonscher redefine the constitutive equation (2.1) along these lines with

$$\chi(\omega) = \epsilon(\omega) - \epsilon_\infty \tag{2.11}$$

where $\omega_p = 1/\tau$ and $\chi(\omega) = \chi(0)F(\omega/\omega_p)$. $F(\omega/\omega_p)$ is referred to as a spectral function and the exponents $\alpha, \beta, \Delta, \gamma$, m and, n as spectral parameters. The functions $F(\omega/\omega_p)$ are displayed in the second column of Table 2.

Galiyarova reviewed many of these various forms in Reference [20] but used the notation $e^* = (\epsilon^* - \epsilon_\infty)/(\epsilon_s - \epsilon_\infty)$, so that $e^* = F(\omega/\omega_p)$. Using this convenient form, the Cole-Cole form, Equation 2.5, can be written

$$e^* = \left(1 + (i\omega\tau)^{1-\alpha}\right)^{-1}. \tag{2.12}$$

The other spectral functions in Table 2 follow. This notation avoids the confusion induced in redefining the constitutive equation.

The assumptions that both the high and low frequency responses are purely capacitive are difficult, if not impossible, to verify in practice. At the high frequency end, phonon and other interactions can mask the polarization response and ϵ_∞ becomes a parameter estimated from graphical analysis of the Cole-Cole plot or through numerical Kramers-Kronig transform calculations. At the low end ϵ_s is more often than not mixed with conductivity.

Table 2. Spectral Functions and Their Power-Law Exponents.

Model	Function*	exponent $\omega << \omega_p$ $\Delta\chi'(\omega)$	exponent $\omega << \omega_p$ $\chi''(\omega)$	exponent $\omega >> \omega_p$ $\chi'(\omega)$	exponent $\omega >> \omega_p$ $\chi''(\omega)$
One parameter					
Debye	$(1+i\omega/\omega_p)^{-1}$	2.0	1.0	-2.0	-1.0
Cole-Cole	$(1+\{i\omega/\omega_p\}^{1-\alpha})^{-1}$	$1-\alpha$	$1-\alpha$	$\alpha-1$	$\alpha-1$
Fuoss-Kirkwood†	$2(\omega/\omega_p)^{\gamma}(1+\{\omega/\omega_p\}^{2\gamma})^{-1}$	γ	γ	$-\gamma$	$-\gamma$
Davidson-Cole	$(1+i\omega/\omega_p)^{-\beta}$	2.0	2.0	$-\beta$	$-\beta$
Williams-Watts	$\sum_{s=1}^{\infty}\frac{\Gamma(\Delta s)}{(s-1)!}\left\|\frac{\exp(-i\Delta\pi/2)}{\omega^{\Delta}\omega_p^{-\Delta}}\right\|^s$	2.0	1.0	$-\Delta$	$-\Delta$
Two parameter					
Havriliak-Negami	$\{1+(i\omega/\omega_p)^{(1-\alpha)}\}^{-\beta}$	$1-\alpha$	$1-\alpha$	$-\beta(1-\alpha)$	$-\beta(1-\alpha)$
Jonscher	$\{(\omega/\omega_1)^{-m}+(\omega/\omega_2)^{1-n}\}^{-1}$	m	m	$n-1$	$n-1$
Hill	$\omega^m(\omega_p^{2s}+\omega^{2s})^{-(m+1-n)/2s}$	m	m	$n-1$	$n-1$
Dissado-Hill	$\{\omega_p/(\omega_p+i\omega)\}^{(1-n)}\,{}_2F_1\left(1-n,1-m;2-n;\frac{\omega_p}{\omega_p+i\omega}\right)$	m	m	$n-1$	$n-1$

*All the spectral parameters are fractional and positive.
†The Fuoss-Kirkwood relationship gives only the imaginary component $\chi''(\omega)$.
Taken from Reference [11]

Low-Frequency, Long-Time Anomalies

Overwhelming experimental evidence indicates that at low enough frequency, or long enough times, all materials, even the best insulators, appear to be conductive to some extent. True, linear resistor-like, conductivity would show up on the Cole-Cole type plots as a vertical line at the lowest frequencies. This represents an ideal limiting case and is often only approximated in nature. The slope of the low-frequency tail varies with composition, temperature and other conditions. Some authors suggest that the low frequency tail could be due to electrode interface effects, although this is still controversial. [4]

Typical permittivity measurements result in a plot such as shown in Figure 9.

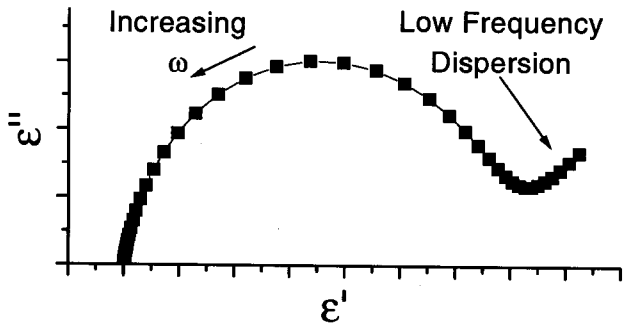

Figure 9. A schematic representation of a typical data set from measurements of a ferroelectric material.

Extensive studies of the very low-frequency, long-time, permittivity behavior of a wide variety of dielectric materials follows the form

$$\epsilon(\omega) \sim \omega^{n-1}, \tag{2.13}$$

where $0 < \eta < 1$. For solid-like materials $\eta \gtrsim 0.6$ and $\eta \sim 0.3 - 0.5$ for liquid-like materials. [2] The cause of this low-frequency dispersion is still an open question (see e.g. [21, 22]).

In the Debye model, the charging and discharging currents are simply opposite in sign but have the same time dependence. This is controversial. In Reference [23], Kumar states that there is a depolarizing current $i_d(t) \sim t^{-\eta}$ after removal of the the polarizing field. This would imply an infinite polarizability of matter if the relation held for all t. In Reference [19], Westerlund states that the current $i_d \sim t^{-\eta}$ is the relaxation response current at long times after the polarizing field is applied. He models the response as a time varying capacitance and attributes long-time dielectric breakdown to the material exceeding some limiting charge capacity. Many articles addressing this low frequency response fail to distinguish between the relaxation after application of the field versus after removal of the field.

The differences between the charging and discharging currents upon application of a pulse of finite duration were predicted by Jonscher in Reference [8] according to the following argument. Experimentally, for the vast majority of dielectric materials, the charging current asymptotically follows a power-law of the form $i \propto t^{-\eta}$. If superposition applies, then a square pulse of duration T could be considered to be a field of +A being turned on at time $t = -T$ and staying on forever with another field of -A being turned on at $t = 0$. The asymptotic current should then be the sum of

the two response currents for $t > 0$:

$$i(t) \propto (T+t)^{-\eta} - t^{-\eta} \tag{2.14}$$

and in the limit of short times, $t \ll T$

$$i(t) \propto t^{-\eta} \tag{2.15}$$

since the first term is negligible in comparison with the second in Equation 2.14. In the limit of long times, $t \gg T$,

$$i(t) \propto t^{-\eta} \left\{ \left(1 + \frac{T}{t}\right)^{-\eta} - 1 \right\} \simeq \eta T t^{-\eta-1}. \tag{2.16}$$

Jonscher was worried that the discharge currents after a pulse of finite duration would only follow the "genuine" characteristics of the material in question for a very short time. He predicted the cross over time for the discharge current to change from $-\eta$ to $-1-\eta$, which would allow the measurement of η from discharge currents.

Polarization versus Conductivity

According to the relations in Table 1, the permittivity function ϵ includes all of the integrated current through the material, due to conductivity as well as the charge stored due to internal polarization. As discussed above it is desirable to "subtract out" the conductivity in order to model the "actual" polarization, i.e. charge stored across the dielectric. Unfortunately, the conductivity is not readily determined from the low-frequency tail of the permittivity, so it is not at all certain what should be

subtracted, especially when different authors refer to the low-frequency response as a time varying conduction and others as a time varying capacitance.

It bears remembering that the plots shown above are for fixed electrical boundary conditions. This leads to a substantial question: with the anomalous conductivity evident in the typical case, how does the voltage across the device behave in the open circuit case? In other words, can we discern the internal leakage from the standard permittivity measurements? This question applies equally to any of the other immitance functions as well.

In line with the thrust of this investigation: does the open circuit relaxation bear any relation to the parameters in the fixed field case? Does it show power-law decay as well? Exploring this question will probably require significant finesse in experimental technique. See chapter 8 for additional discussion.

From Whence the Power-law?

Numerous models for the causes of the memory effect have been postulated. For example, in Reference [24], Ngai and Rajagopal postulated that the time dependent transition rates giving rise to non-Debye relaxation are due to the interaction with the heat bath. In this theory, the low-energy level spacings of the heat bath determine the long-time relaxation process. It is difficult to see how the concentration of a dipolar liquid would cause variation in the long-time response if the rate were determined by interaction with the environment as opposed to internal interactions. Additionally,

this model predicts stretched exponential response, not power-law. Other models, mostly based on some fixed distribution of defects within the material, predict power-law behavior over only a limited frequency range.

Given the universal nature of the power-law forms of the observed relaxation processes in solids and non-dilute liquids, it may be reasonable to suspect that it is a natural consequence of a many body problem. The polarization can be viewed as being due to bound charge carriers hopping to between states with different charge symmetries than their ground states. In addition to the possibility that the charged particles might undergo relaxation back to the original states, it may be possible for the local environments to relax around the new states, reducing the likelihood of the return to the ground states. These metastable states may have lifetimes many orders of magnitude greater than that which would occur if the environments had not been modified. These metastable states may again interact with one another and form new relaxation conditions leading to the observed "distribution of decay times."

One major new possibility comes into play: the distribution of the trapping times may be such that the second moments diverge. In this case, the canonical central limit theorem no longer holds. That is, the statistics are not necessarily Gaussian. Instead, a Lévy, or α-Stable, distribution can result. The Lévy distribution is noted for its long power-law tails. These divergent tailed distributions percolate their way up to the macroscopic scale as a long-time power-law memory. A similar argument for conductive response can be made. These models will be discussed in some detail in

Chapter 3. The natural mathematics of power-law relations is the fractional calculus, which will be discussed in Chapter 4.

If the power-law relations represent true memory effects and are not just convenient curve fitting parameters, then there must be an intimate relation between the *ac* and *dc* response in any given material represented by a dynamical equation of motion. It should be possible to associate variation of parameters in a power-law model with variation in composition and boundary conditions.

Hypothesis

Hypothesis: *Dielectric dynamics can be accurately modeled using the fractional calculus.*

- Included in the hypothesis is that the low-frequency, long-time tails in the permittivity must also be accounted for via a memory function in the fractional calculus model.
- The testing of the hypothesis will begin with development of numerical techniques for dealing with non-Markovian differential equations represented in the fractional calculus. This will then allow for comparison of predictions of time domain response generated from modeling, using data obtained in the frequency domain, with measured time domain response for a variety of materials under a variety of conditions.

- For the hypothesis to be falsified, either the *ac* measurements should substantially deviate from power-law behavior or the time domain response should deviate from that predicted by the model developed from the *ac* response.
- For the hypothesis to be rendered non-applicable, the exponents and coefficients should show no discernible pattern of variation as a result of incremental changes in composition or boundary conditions.

CHAPTER 3

THE MODEL

The composite model for dielectric relaxation to be discussed in this Chapter is based on ideas by Hill and Jonscher [11], Funke [12] and Bouchaud and Georges [25]. In each of these cited references, the assumption is made that the bound or mobile charge carriers hop or move about in an environment that interacts with the charge carrier. That is, the local energy potential landscape is not independent of the motion of the charge carriers.

Stated more precisely, these models consistently drop the assumption that there is some defect structure inherent in the material with some fixed distribution of trapping times or energies. Rather, the defect structure is seen to be a direct result of the dynamics of the polarization or conduction. The result is an "annealed" as opposed to "quenched" disorder in the material.

Polarization and Conduction as Statistical Quantities

Polarization and conduction in bulk materials are statistical quantities representing the sum of a large number of contributions from the motion of bound or mobile charge carriers. Viewing ideal conductivity as a friction limited drift under an external force (the applied field), the current should depend linearly on the field and therefore

be constant under constant field. Viewing polarization as purely bound charge, the current should fall to zero exponentially after application of a field. As pointed out in the previous chapter, neither of these ideal behaviors are seen. Instead, power-law relations in time and frequency are the norm. Indeed, Westerlund [17] reported that after measuring "tens of thousands of capacitors of all types and makes," every unit exhibited "anomalous" behavior.

As limits of sums of statistical distributions, the bulk quantities of polarization and conductivity should have statistics which obey the law of large numbers, and the central limit theorem (CLT), at first glance, should require that the sum of independent random variables converges to a Gaussian distribution. Linear systems are expected to exhibit exponential relaxation dynamics. Why then are non-Gaussian and non-exponential behaviors so ubiquitous even in the small signal, linear response regime?

A Statistical Digression

To adequately address the question raised above, it will be necessary to review the law of large numbers and the central limit theorem to see when they apply and when they break down. In what follows, we assume that the material is homogeneous so that a single statistical distribution can be used to describe the behavior of a given process throughout the sample. One material may exhibit a number of different processes, but, this number of distinctly different processes is assumed to be small.

The competition among these processes will be discussed later. For now, we discuss one process at a time.

The law of large numbers states that average of a set of measurements will converge to the mean of a distribution if the mean exists. This law does not depend on the existence of a variance or second moment of the distribution. It is the law of large numbers that allows us to treat fundamentally statistical processes such as the flow of current as deterministic events at the macroscopic scale. The canonical central limit theorem, however, does depend on the existence of a second moment.

As discussed in more detail in Appendix A, the canonical central limit theorem depends on two fundamental assumptions; first that the distributions of the contributing events have a convergent second moment, and, second, that the events contributing to the the sum are adequately independent. We are most concerned with the failure of the first assumption here. Failure of the second assumption will be discussed in Appendix B.

There is a generalized central limit theorem which states that if the events are adequately independent, but have tails to the probability distribution that fall off slower than $t^{-1-\alpha}$, where $2 < \alpha < 0$, then the limit (sum) distribution will have the form of a Lévy, or α-stable, distribution with its characteristic power-law tails. The implication here is that the power-law tails show up in a macroscopic way in the sum distribution. In the case of divergent waiting times to be discussed here, it means that the polarization and current dynamics will exhibit power-law behavior. Further, we

expect that the exponents for the response under an applied field and the relaxation response in the absence of a field will be different.

Polarization

Hill and Jonscher suggested that the power-law behavior in dielectrics should be considered a consequence of the many-body interactions making up bulk condensed matter. A model formalizing this idea and reproducing the Cole-Cole plot (Figure 4) over a broad range of frequencies was proposed by Funke [12]. The basic premise is that the potential energy landscape creating the double- or multi-well potential of a bound charge is not independent of the motion of the charge.

Figure 10 provides a schematic of the hop processes proposed by Funke. In addition to the possibility that an excited particle could relax by returning to the ground state directly, there is the possibility that the local environment could relax. In Figure 10 this is represented by the energy profile relaxing from curve (a) to curve (b) and the particle undergoing the "transition" indicated by process (3). In this case, the time to return to the ground state, process (2), can be many orders of magnitude greater than that predicted by the Debye theory, which accounts for only this possibility. Funke's result is independent of any specific model of relaxation of the environment and will not be reproduced here. All that is needed is that the distribution of waiting times for return to the ground state, i.e. jump process (2), fall off slower than t^{-3}.

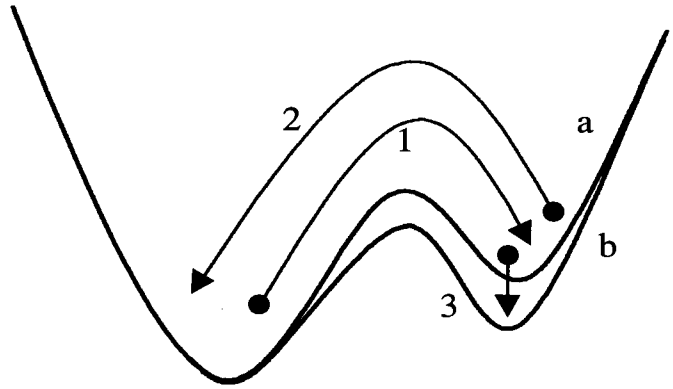

Figure 10. A schematic representation of the bound charge hopping model. The initial potential landscape is represented by curve (a). After a hop to the right (1), the particle can relax back to the initial state (2), or the environment can relax to curve (b) reducing the energy (3) resulting in reduced likelihood of return to the ground state.

Funke places several limitations on the theory, which now appear to be unnecessary. First, there is the assumption that the Cole-Cole curve must make a vertical approach to the real axis on the ϵ'' vs. ϵ' plot at both the highest and lowest frequencies. Second, the low-frequency dispersion is out-of-hand relegated to a surface effect and unrelated to the bulk response. Neither of these assumptions were justified in Reference [12].

Conductivity

A model for frequency dependent conductivity, the "universal dielectric response," was proposed by Bouchaud and Georges [25]. This model is in many ways an extension of that of Funke. Mobile charge carriers interact with defects formed by the creation of carriers in the first place. This is necessarily a dynamic effect. Again, the trapping

of the mobile charges by these defects is a dynamic process and the local environment is given the opportunity to relax around the defect and a charge carrier can be trapped in the defect. Again there is the possibility of a divergent waiting time for escape from the trap. In this model the mobility follows a power law $m(\omega) \sim (i\omega)^{\alpha}$. This power law is the source of the memory. The longer a trapping site lasts, the longer it is likely to last. In addition, it is more likely to affect sites in the local neighborhood. This results in what has been referred to as a "self-pinning" effect. This cooperative relaxation may also result in the observed remanent domain structures seen in ferroelectric materials.

There are issues with respect to the dimensionality of the problem, but, for this work, we consider primarily polarization and conduction along a single principal axis at a time and ignore the tensor nature of the problem.

It has been shown that the "universal dielectric response" is expected to produce 1/f noise. [26]. It is important to note that the model of dynamic disorder described above fits extremely well with other models of 1/f noise production in that very carefully prepared pure materials generate the least noise, while the level of noise grows with increasing "ab initio," or "quenched," disorder.

Competition and Mixing

From the experimental data reported in the literature, it is likely that there will be several competing bound and mobile charge carrying processes going on within any

material. If we are lucky, these will have sufficiently different distributions of waiting times and the effects of each will be distinct. The composite model permittivity will then contain terms proportional to the electric field times a strength factor, ϵ_i and fractional frequency dependence $(i\omega)^{\alpha_i}$, where, in general, the exponent α_i depends on whether the process represents a bound or mobile charge response to the field. In addition, there will be a polarization relaxation term proportional to $(i\omega)^q$, where $q = 1 - \alpha$ from the Funke model to account for the relaxation upon removal of the external field. Each of these, in turn, will be interpreted as a Laplace transform of a fractional derivative operator of the form ${}_0D_t^q$ to be described in the next chapter.

An open question is whether or not the competition between and among processes can lead to mixing of exponents. One of the models to be derived in Chapter 5 treats the exponents as separate entities while another allows such mixing.

There is still no detailed microscopic description of polarization that produces the CPE behavior. There is still some ambiguity as to whether the low-frequency dispersion is due to interface effects between the electrodes and the dielectric or whether it originates within the bulk of the dielectric or both.

Distributions of Relaxation Times

While this chapter has concentrated on the statistical description of power-law dynamics, it should be noted that the theory of distributions of relaxation times has made complementary progress as well. Reference [10] provides a description

of multifractal functions of the distribution for Cole-Cole, Havriliak-Negami, and Davidson-Cole relaxation processes. Analysis of these functions as thermodynamic entities reveals the competition between processes with different time scales. The discovery of phase transitions in multifractal analysis is a new development and, as the authors of Reference [10] point out, there are many unanswered questions. It may turn out that further advances on both fronts will lead to development of more specific models. In both the fractional-time power-law and fractal-time distribution models, the creation of the exponents and the divergence of the distributions are due to the macroscopic sum of an enormous number of contributing microscopic activities.

A Plethora of Models?

Any of the forms in Table 2 may be used as a starting point for development of a spectral permittivity function, but the models proposed here abandon the assumption that the high and low frequency terms must necessarily be represented by purely real permittivity terms. The result of this is that any proposed equivalent circuit element, resistor or capacitor, should be replaced with an appropriate constant phase element (CPE) as described in Chapter 2. This process will be undertaken in Chapter 5 where two specific model forms are developed.

CHAPTER 4

THE FRACTIONAL CALCULUS

The fractional calculus is the natural mathematical language of power-law relations and has been proposed by a number of authors as being applicable to the problem of power-law relaxation dynamics. While frequency domain plots of dielectric response have been accurately fit with power-law equations, it has yet to be shown that the fits truly represent fractional differential equations capable of predicting time domain transients. This chapter introduces some basic concepts of the fractional calculus that will be required in later chapters.

The fractional calculus dates from very shortly after the classical calculus became known; Leibniz mentioned it in a letter to L'Hopital in 1695. Euler and Lagrange made significant contributions with the more systematic treatment credited to Liouville, Riemann and Holmgren in the mid-19th century. Somewhat different definitions exist today but translations are tabulated in texts and have to do mainly with composition rules and treatment of initial conditions. The two most useful texts, References [27] and [28], are unfortunately out of print. Also useful for analytic manipulation of fractional differential equations is Mathai and Saxena's text on the Fox function. [29] More recently Podlubny [30] discussed a number of techniques for attacking fractional differential equations including rudimentary numerical methods.

While the name "differentiation and integration to arbitrary order" may be more accurate, "fractional calculus" is the term that is generally used. Nonetheless, the order is arbitrary and not limited to the set of rational numbers.

The Definition of the Fractional Derivative

This section on the definition of the fractional derivative presents excerpts from Chapter 3 of Reference [27].

The fractional order derivative can be motivated via the standard integer order derivative, which can be defined via Cauchy's integral formula:

$$\frac{\mathrm{d}^{\mathrm{n}}}{\mathrm{dz}^{\mathrm{n}}} f\left(z\right) = \frac{n!}{2\pi i} \oint_C \frac{f(\zeta) d\zeta}{\left[\zeta - z\right]^{n+1}} \tag{4.1}$$

where C describes a closed contour in the complex plane surrounding the point z and enclosing a region of analyticity of the function f. When the positive integer n is replaced be a non-integer q, then $[\zeta - z]^{-q-1}$ no longer has a pole at $\zeta = z$ but a branch point. One is no longer free to deform the contour C surrounding z, since the integral will depend on the location of the point at which C crosses the branch line for $[\zeta - z]^{-q-1}$. The point of origin is chosen to be 0 and the branch line to be the straight line joining 0 and z and continuing indefinitely in the quadrant Re $(\zeta) \leq 0$, $\mathrm{Im}(\zeta) \leq 0$. Then one simply defines, for q not an integer,

$$\frac{\mathrm{d}^{\mathrm{q}}}{\mathrm{dz}^{\mathrm{q}}} f\left(z\right) = \frac{\Gamma(q+1)}{2\pi i} \oint_C \frac{f(\zeta) d\zeta}{\left[\zeta - z\right]^{q+1}}, \tag{4.2}$$

where the contour C begins and ends at $\zeta = 0$ enclosing z once in the positive sense.

The Gamma function, $\Gamma()$, is the generalized factorial function described in Chapter 6 of Reference [31].

To uniquely specify the denominator of the integrand, one defines

$$[\zeta - z]^{q+1} = \exp\left([q+1]\ln(\zeta - z)\right), \tag{4.3}$$

where $\ln(\zeta - z)$ is real when $\zeta - z > 0$. Equation 4.2 can be simplified as

$$\begin{aligned}\frac{\Gamma(q+1)}{2\pi i}\oint_C \frac{f(\zeta)d\zeta}{[\zeta - z]^{q+1}} &= \frac{\Gamma(q+1)}{2\pi i}\left[1 - \exp(-2\pi i[q+1])\right]\int_0^z \frac{f(\zeta)d\zeta}{[\zeta - z]^{q+1}} \\ &= \frac{1}{\Gamma(-q)}\int_0^z \frac{f(\zeta)d\zeta}{[\zeta - z]^{q+1}}.\end{aligned} \tag{4.4}$$

This definition has been attributed to Nekrassov (1888).

The Riemann-Liouville definition is

$$\left[\frac{d^q f}{d(x-a)^q}\right] = \frac{1}{\Gamma(-q)}\int_a^x [x-y]^{-q-1} f(y)dy, \quad q < 0, \tag{4.5}$$

which extends the Nekrassov definition to a non-zero starting point. The Riemann-Liouville definition is of considerable interest in analytical methods but has notoriously bad numerical convergence.

A more useful definition for numerical application was first given by Grünwald (1867) and later extended by Post (1930). Derivatives (of positive order q) or integrals (of negative order q) can be defined by the formula

$$\frac{\mathrm{d}^{\mathrm{q}}}{\mathrm{d(t-a)^q}} f(t) = \lim_{N\to\infty}\left\{\frac{\left[\frac{t-a}{N}\right]^{-q}}{\Gamma(-q)}\sum_{j=0}^{N-1}\frac{\Gamma(j-q)}{\Gamma(j+1)} f\left(t - j\left[\frac{t-a}{N}\right]\right)\right\}, \tag{4.6}$$

where q is arbitrary. Due to the fact that the definition is continuous in q, it is sometimes given the name "differintegral" to imply that it applies to both derivatives

and integrals in the classical sense. This definition exhibits excellent numerical convergence for finite N, thus allowing use in finite difference methods. The Grünwald definition, Equation 4.6, can be shown to be completely equivalent to the Riemann-Liouville definition, Equation 4.5.

A notable difficulty is that the fractional derivative is "non-local" as it is defined over a finite interval, between a and x, where $x > a$. Note that the differential step size, dt, is defined via $(t-a)/N$ just as it is in integer order calculus for integrals. Evaluation at the point $x = a$ is specifically excluded. In the limit of $q \to n$, n a positive integer, all but $n+1$ of the terms of the sum in Equation 4.6 go to zero. In this case, as $N \to \infty$, only the most immediate past is incorporated into the computation and the definition becomes "local." For non-integer q, the weighting factors, $\Gamma(j-q)/(\Gamma(-q)\Gamma(j+1))$, scale as a power-law in j for large j. This weights prior history, back to the beginning of the interval, with a power law in time. Only for integer q does the derivative have geometric meaning in the sense of slope or curvature "at a point."

A example of the weights involved in the fractional derivative, for $q = 0.5$, is shown in Figures 11 and 12. The fractional derivative is found by taking the sum of the products of the function value times the weight times dt^{-q}.

This power-law weighting of history is how the mathematics reflects the physics of power-law relaxation processes. The limit of q approaching an integer represents a process with a finite second moment of the waiting time distribution. When q is

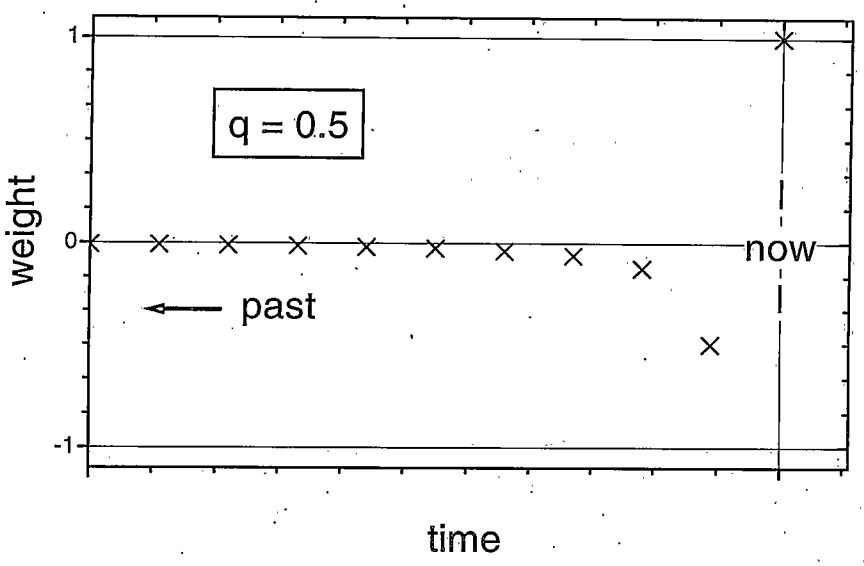

Figure 11. Linear plot of weights associated with the fractional derivative for $q = 0{,}5$.

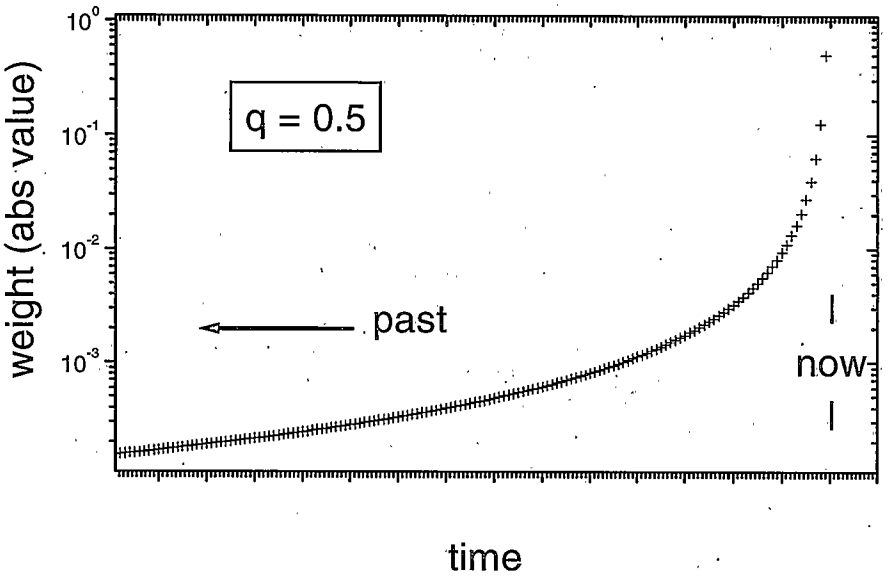

Figure 12. Logarithmic plot of the absolute value of the weights associated with the fractional derivative for $q = 0.5$. The time scale shown here is 15 times longer than that shown in Figure 11.

not an integer, an infinite amount of information is required to accurately produce the fractional derivative. The problem then fails to meet the criteria for a Markov process and we are faced with a fundamentally non-Markovian process. [32] While finite difference equations can be used for some purposes, as will be developed in subsequent chapters, we will always be losing information.

The notation used in fractional calculus has been adapted for the differintegral requiring specification of the interval for both positive and negative orders. In the older notation used by Oldham and Spanier in Reference [27], $\mathrm{d}^q/[\mathrm{d}(t-a)]^q$ indicates that the interval is from a to t. The modern notation, used by Miller and Ross [28], is ${}_aD_t^q$.

A second notable difficulty with the fractional order derivative is that the derivative of a nonzero constant is not zero. This is a direct consequence of the branch cut required in the definition. For example, the derivative of unity is:

$$\frac{\mathrm{d}^q[1]}{[\mathrm{d}(t-a)]^q} = {}_aD_t^q[1] = \lim_{N\to\infty}\left\{\left[\frac{N}{t-a}\right]^q \frac{\Gamma(N-q)}{\Gamma(1-q)\Gamma(N)}\right\} = \frac{[t-a]^{-q}}{\Gamma(1-q)} \tag{4.7}$$

The fractional differintegral is a linear operator. The Laplace transform applies to fractional real and reciprocal space variables continuously in all orders of q. The Mellin transform,

$$\mathcal{M}\{f(t);s\} = \int_0^\infty f(t)t^{s-1}dt, \tag{4.8}$$

finds extensive use in fractional analysis due to its power-law transform kernel. Green's function methods have also been developed for use with fractional calculus.

As with integer order calculus, care must be taken when forming compositions of operators. For example, the integral of a derivative of a function differs from the derivative of the integral of the function by the value of any terms taken to zero by the differentiation in the first case. With integer order calculus this problem is addressed through the addition of constants of integration. In the fractional case, the initial conditions result in the inclusion of terms such as Equation 4.7 for both derivatives and integrals. The rules get rather complicated and the reader is referred to texts such as [27] and [28] for the details.

Causality and Time Inversion

Since the fractional differintegral operates over the interval $(-\infty, t)$, it satisfies causality by construction. It is this property that guarantees that response functions based on fractional differintegrals will satisfy the Kramers-Kronig relations. The fractional differintegral operator is not symmetric with respect to time inversion, and so the dynamics are irreversible and will not generally conserve energy.

Fractional Derivative of a Sinusoid

Since much of what follows in the next two chapters involves *ac* responses, we will need the fractional derivative of a sinusoid, which is

$$\frac{\mathrm{d}^q}{\mathrm{d}t^q}\sin(\omega t) = {}_0D_t^q \sin(\omega t) = \omega^q \sin(\omega t + q\frac{\pi}{2}) + \ \textit{transient terms.} \qquad (4.9)$$

That the fractional derivative operator is linear means that superposition holds and no

additional frequency components are generated in a fractional process. The fractional derivative converges to the integer order result as the exponent approaches an integer value. Note that the phase angle is independent of frequency, i.e. a "constant phase element." The frequency independent loss factor discussed in Chapter 2 is seen as a direct result of the memory function.

The transient terms are complicated, but can generally be described as a combination of a power-law decaying bias plus a power-law decaying oscillation. In combination they can produce an apparent phase drift with the phase settling to $q\pi/2$ asymptotically. Since the phase accuracy is potentially in question, both the numerical simulations and experimental measurements will allow for long (in terms of τ) waiting periods after initiating an *ac* field.

Fractional Relaxation

The problem of non-exponential relaxation illustrates some of the methods of fractional calculus. It is often the case that fractional differential equations can be developed from generalizations of integer order systems.

Following Glöckle and Nonnenmacher [33], simple first order relaxation can be written

$$(1 + \tau\, {}_0D_t)\, \phi(t) = 0. \tag{4.10}$$

or:

$$\dot{\phi}(t) = -\frac{1}{\tau}\phi(t), \tag{4.11}$$

where $\phi(t)$ represents a physical variable such as electrical polarization or mechanical strain. The solution is

$$\phi(t) = \phi_0 - \frac{1}{\tau}\int_0^t \phi(t')\mathrm{d}t'. \tag{4.12}$$

We can generalize the system to allow non-exponential response by replacing the Riemann integral operator (the anti-derivative) $(1/\tau)\,{}_0D_t^{-1}$ with $(1/\tau)^q\,{}_0D_t^{-q}$, to obtain

$$\phi(t) - \phi_0 = -\frac{1}{\tau^q}\,{}_0D_t^{-q}\phi(t). \tag{4.13}$$

Applying $\tau^q{}_0D_t^q$ from the right and using the differential rule for a constant, ${}_0D_t^{-q}\phi_0 = \phi_0 t^{-q}/\Gamma(1-q)$, results in

$${}_0D_t^q\phi(t) - \phi_0\frac{t^{-q}}{\Gamma(1-q)} = -\tau^{-q}\phi(t). \tag{4.14}$$

From here, we apply the Laplace transform, leading to

$$\tilde{\phi}(s) = \phi_0\frac{s^{-1}}{1+(s\tau)^{-q}}. \tag{4.15}$$

Looking up this form in a reference (e.g. [29]), we find the series expansion

$$\phi(t) = \phi_0\sum_{k=0}^{\infty}\frac{(-1)^k}{\Gamma(1+qk)}\left(\frac{t}{\tau}\right)^{qk}, \tag{4.16}$$

from which we recover the exponential in the limit $q \to 1$.

Time domain plots of Equation 4.16 with various values of q are shown in Figure 13. Even for values of the exponent near unity, there is still a transition to power law behavior after some time. Note that the solution is, in fact, dominated by the initial condition at short times and can be fit quite well with a "stretched exponential" for $t \sim \tau$.

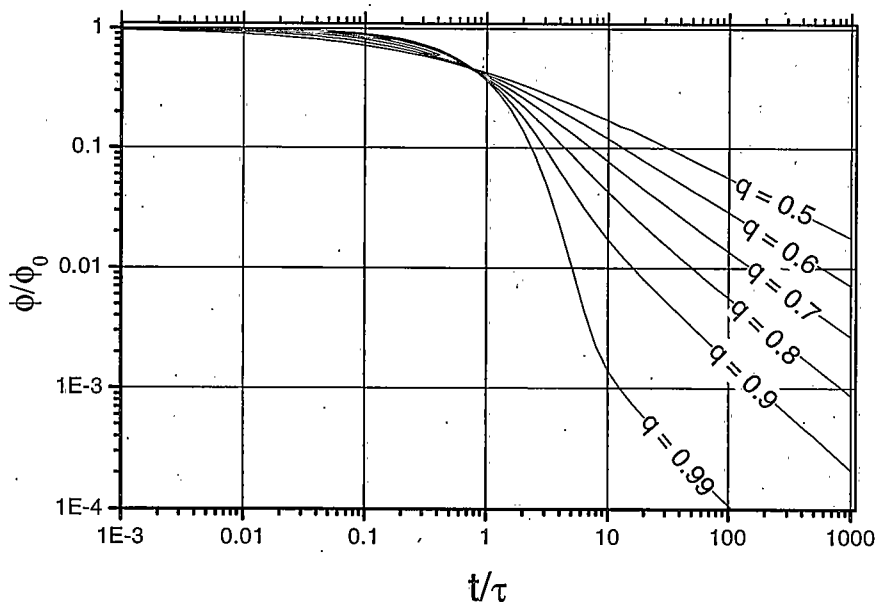

Figure 13. Time domain decay of polarization for various values of the exponent q.

The derivation above actually represents an overly idealized situation and can be misleading. The initial condition ignores the history of how the initial polarization or strain was achieved. For the fractional calculus to provide a meaningful model of dynamic behavior, the fractional derivative operator must include the entire history from the last moment that the field and response were both zero. Since this is not

feasible with the analytical methods currently available, a major effort of this work was dedicated to the development of numerical methods to allow exploration of the effect of imposing a arbitrary field of finite duration. The results of this effort will be presented in Chapter 6.

CHAPTER 5

DERIVATION OF THE DIFFERENTIAL EQUATION

A major step in constructing a consistent model of polarization dynamics is the development of a time domain differential equation. This will be carried out by generalizing models of ideal circuit elements, e.g. the Debye behavior, and adding low frequency conductivity. As discussed in Chapter 3, any of the forms in Table 2 could be used as a starting point. Alternatively, an equivalent circuit could be proposed and selected resistors and/or capacitors could be replaced with CPE. One of each is developed here: one generalizing the Cole-Cole model directly and the other by generalizing the impedance function of a circuit model. Both dynamical models incorporate both a dielectric loss peak and low-frequency dispersion.

Other models can be proposed, each potentially suffering from the act of attempting to obtain the general case from an ideal equivalent circuit model. The thrust of future experimental work will be to attempt to eliminate incorrect models.

Much of the methodology used in this chapter was motivated by Reference [34] which suggests application of the fractional calculus to the problem of relaxation in mechanical systems. While the idea of applying the fractional calculus to the description of dielectric response is not new, the work presented here is unique in that it incorporates (almost) all of the dynamics of the dielectric response over an

extended range of frequencies and times. Additionally, the models developed as part of this research will allow comparison between *ac* and *dc* responses, which was an objective outlined in Chapter 1.

As will be seen, the caveat "almost" above applies to the fact that a piezoelectric resonance will be seen in the spectral response of PVDF that is not taken into account, as yet, in the models presented.

The Permittivity Equation

We can construct a form of the constitutive equation relating the polarization to the applied field, by starting with the electric displacement,

$$\mathbf{D}(t) = \epsilon_0 \mathbf{E}(t) + \epsilon_0 \int_{-\infty}^{\infty} f(\tau)\mathbf{E}(t-\tau)\mathrm{d}\tau, \quad \text{with } f(\tau) = 0 \text{ for } \tau < 0, \tag{5.1}$$

where $f(t)$ represents a memory function associated with the material properties of the dielectric. [35] This convolution in the time domain becomes a simple product of functions in the frequency domain. With $\mathbf{D}(\omega) = (1 + \chi_e(\omega))\epsilon_0\mathbf{E}(\omega)$ and $\mathbf{P}(\omega) = \chi_e(\omega)\epsilon_0\mathbf{E}(\omega)$, we see that

$$\chi_e(\omega) = \int_{-\infty}^{\infty} f(\tau)e^{i\omega\tau}\mathrm{d}\tau. \tag{5.2}$$

In words, $\chi_e(\omega)$ is just the Fourier transform of the memory function. Since χ_e is often on the order of 10 or greater for dielectric materials of interest, it is customary to equate $\epsilon(\omega)$ and $\chi_e(\omega)$. With this approximation, $\epsilon(\omega)$ can be interpreted as the limiting case, $s \to i\omega$, of the Laplace transfer function $\mathbf{P}(\mathrm{s})/\mathbf{E}(\mathrm{s})$.

It is important to note that the expectation should be that the polarization response depends on the entire past history of the the applied field.[36] Power law behavior is the simplest non-exponential response that incorporates the memory effect.

We can begin to see how to incorporate memory by viewing the Debye formula as the limiting case of a Laplace transfer function and inverting it to form a time domain differential equation:

$$\mathbf{P}(t) + \tau \frac{\partial}{\partial t}\mathbf{P}(t) = \epsilon_s \mathbf{E}(t) + \epsilon_\infty \tau \frac{\partial}{\partial t}\mathbf{E}(t). \tag{5.3}$$

Applying the Fractional Calculus to Non-exponential Processes

Interpretation of complex permittivity plots using power-law fitting dates back to Cole and Cole [3]. In terms of the complex conjugate of the permittivity $\epsilon^* = \epsilon' - i\epsilon''$, simple Debye relaxation would appear as a semicircle on a plot of ϵ'' versus ϵ'. [1] Written in traditional form:

$$\epsilon^* - \epsilon_\infty = \frac{\epsilon_s - \epsilon_\infty}{1 + i\omega\tau} \quad \text{(Debye)} \tag{5.4}$$

The use of the complex conjugate ϵ^* places the Cole-Cole plot in the first quadrant.

As stated above, the permittivity, sometimes referred to as the "dielectric constant," is the *relative* permittivity. However, it is often convenient to set the scaling constant ϵ_0 between $\mathbf{D}$ and $\mathbf{E}$ to unity when convenient for computational purposes as will be done here.